High-Power Microwave Filters*

JOSEPH H. VOGELMAN†

Summary—**In order to obtain filters capable of handling very high power, the use of radial lines and uniform line discontinuities was investigated as the most promising approach. In this connection, it was necessary to consider the equivalent circuit and interaction for *H*-type radial line mated at each end to uniform TE_{10} waveguide for taper angles of 45°. It was found that the equivalent circuit was valid for taper angles of 45°, and that for engineering design purposes the interaction could be neglected. The author utilized the 45° tapers and the uniform lines to design a high-power microwave filter capable of handling 700 kw at 10 pounds pressure in 0.900 by 0.400 ID waveguide. The design procedure for a multielement filter is described utilizing a partly graphical approach.**

Introduction

SINCE the introduction of radar in the inventory of the United States Air Force, the problem of spurious radiation from the high-power transmitters and the interfering effects on other radars and on communications has been growing in magnitude. As the power of the radar transmitters increased and the frequency spectrum became increasingly crowded, the mutual interference between radars at the same site or between radars and communication reached critical proportions. Since 1948 a major effort has been underway to reduce the deleterious effects of interference. Pulse radar transmitters have been found to radiate relatively large power at spurious frequencies far removed from the operating frequency. These frequencies frequently occur in the assigned operating band of other radars and communications equipments. Accordingly, it is essential to eliminate the spurious radiation at the transmitter. To remove the spurious radiation, the various filters described in the literature by Cohn [5]–[7], Fano [4] and others were examined for their power handling capability. Since the radars in use transmit peak power of the same order of magnitude as the breakdown power of the waveguide, any filter used may not have dimensions smaller than the normal waveguide itself. An examination of the literature and tests of the more promising types indicated that the designs available were not capable of passing the radar transmitter power without breakdown of serious corona and arcing. A new approach was required. The first filter considered consisted of a series of steps similar to that described by Cohn [5] with the exception that the minimum height of the constricted step was made equal to the normal waveguide height.

This type of filter failed to meet the power handling requirement because of the large gradient at the corners of the steps. Since the author had built feed horns with flared outputs which handled large radar power, it appeared that a filter section made up of flared walls would have promise of handling high peak power. The author built in 1953 [3] a filter section consisting of a waveguide of rectangular cross section whose narrow dimensions were expanded through a taper and then contracted through another taper to its original dimensions. The two tapers were separated by a short length of enlarged uniform line [Fig. 1(a)]. The four discontinuities between the uniform and radial lines have a frequency dependence similar to a heavily loaded resonant cavity. Since the taper to uniform line is a more gradual change than a step, this type filter should have a considerably smaller gradient in the vicinity of the discontinuity, and it should be capable of handling high power. The resultant structure was experimentally examined for its transmission characteristics and found to exhibit the properties of a low *Q* band-pass filter. When tested for power handling, it was found to have approximately the same peak power capacity as the uniform waveguide with the normal *E*- and *H*-plane bends when tested at the frequency of minimum insertion loss. This new microwave circuit offered interesting possibilities. The research to be described was undertaken to investigate and apply this circuit form.

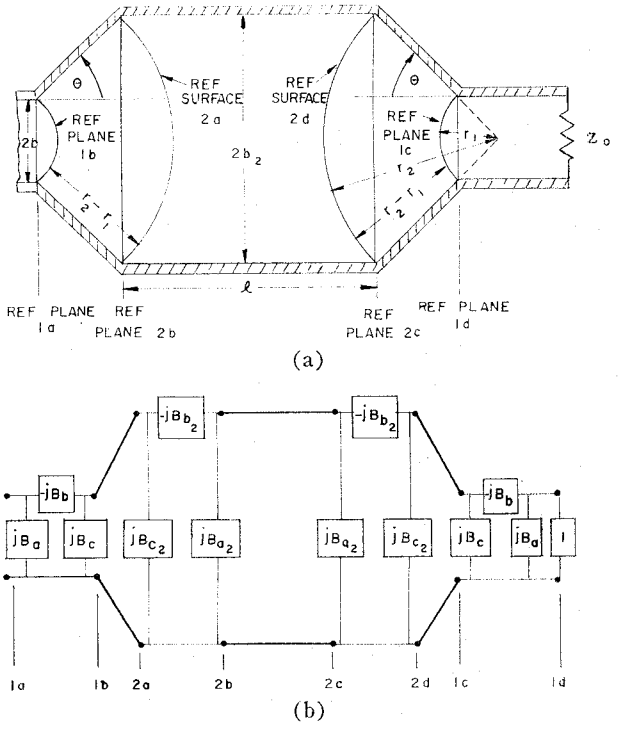

Fig. 1—Physical dimensions and equivalent circuit of a filter section. (a) Physical structure. (b) Equivalent circuit.

* Manuscript received by the PGMTT, May 16, 1958; revised manuscript received, June 30, 1958. The work for this paper was done in partial fulfillment of the requirements for the D.E.E. degree, Polytechnic Inst. Brooklyn, Brooklyn, N. Y., June, 1957.

† Directorate of Communications, Rome Air Dev. Ctr., Griffiss Air Force Base, Rome, N. Y.

Purpose

The main purpose of the research program was intended to furnish adequate analytic description to permit designing and using this microwave circuit in practical applications. The problem resolved itself into two parts:

1) To determine if the equivalent circuit of the "Waveguide Handbook" [1] accurately described the discontinuity between a uniform and an E-plane radial line for taper angles as large as 45°, and if the *interaction* between two adjacent discontinuities in the radial line was small enough to be considered negligible for engineering design purposes.

2) To utilize analytic and experimental properties of tapered sections to derive a rationale for the design of tapered section band-pass and band elimination filters.

Equivalent Circuit of One Discontinuity

The equivalent circuit of the discontinuity resulting from the junction of an axially symmetrical radial line with a uniform waveguide is identical with that resulting from an asymmetrical junction of a radial line having the same angle with respect to the axis and a uniform line of half the height (Fig. 2). The resulting admittances for the equivalent circuit are given by the following equations [1] (normalized to the rectangular waveguide characteristic admittance):

$$B_a = \frac{2\pi b}{\lambda_g \theta} \ln \frac{\theta}{\sin \theta} \tag{1}$$

$$B_b = \frac{\lambda_g}{\pi b} \frac{\sin \theta}{\theta} \frac{\sin \theta}{1 - \dfrac{\sin 2\theta}{2\theta}} \tag{2}$$

$$B_c = \frac{2b}{\lambda_g}\left[0.577 + \psi\left(\frac{\theta}{\pi}\right)\right] \tag{3}$$

$$\psi(\theta/\pi) = \frac{d \ln \Gamma((\theta/\pi) + 1)}{d(\theta/\pi)} .$$

(See Cohn [2].)

Experiments were set up to confirm these results by obtaining experimentally the equivalent circuit and comparing the results.

Interaction Between Adjacent Radial Line Discontinuities

The first experimental results confirmed the accuracy of the equivalent circuit within 1 per cent and established a method for examining experimentally combinations of discontinuities resulting from the junction of uniform and H-type radial waveguides. The second set of experiments and analysis was intended to investigate the interaction between two adjacent discontinuities along the radial line, resulting from higher order modes in this line and to determine the effect of neglecting it for design purposes. The taper angle, $\pi/4$, between the radial wall and the waveguide axis was selected as a compromise between maximum power handling capacity and magnitude of the discontinuity. The discontinuity capacitance increases while the power handling capacity decreases as the angle increases.

These measurements served to provide a basis for proceeding with the design of the filters, considering the interaction as negligible. The validity of this conclusion was confirmed by the correlation between the design calculations and the measured results. [3]

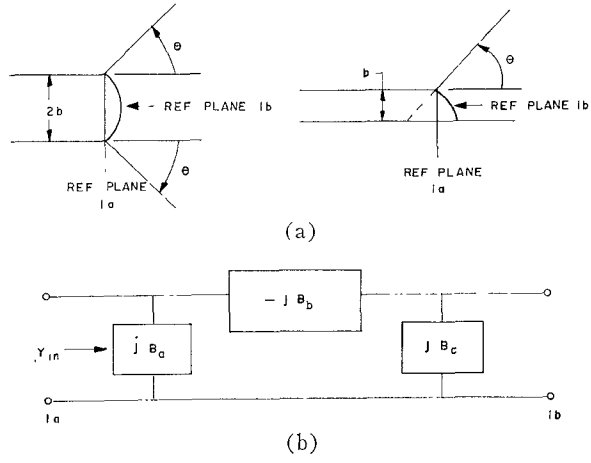

Fig. 2—Junction of uniform and radial line. (a) Physical structure. (b) Equivalent circuit.

The Single Filter Section

A single filter section consisting of two H-type radial lines connected by an enlarged uniform rectangular waveguide will be examined for its characteristics. It will form the fundamental element of a multisection filter design capable of passing high power in one band while providing large loss in the attenuation band.

Equivalent Circuit of a Single-Filter Section

The physical structure to be considered and its equivalent circuit are shown in Fig. 1. Using this equivalent circuit, the equations which describe the insertion loss can be found in terms of the various parameters forming the equivalent circuit. It should be noted that the specific circuit element values change with frequency, and new values are needed for each frequency of operation.

Since H-type radial line and H_{10} rectangular waveguide operation must be described in terms of the waveguide wavelength, a normalizing procedure will be used to make the results generally applicable. Accordingly all dimensions will be normalized to the waveguide wavelength and the parameters x and y as defined by (4a) and (4b) will be used as the variables describing the dimensions of the structure:

$$x = 2\pi r_1/\lambda_g \tag{4a}$$

$$y = 2\pi r_2/\lambda_g \tag{4b}$$

where r_1 and r_2 are defined in Fig. 1.

TABLE I
NORMALIZED SUSCEPTANCES FOR EQUIVALENT CIRCUIT OF UNIFORM TO RADIAL LINE DISCONTINUITY

θ/π	$B_a'(\theta)$	$B_b'(\theta)$	$B_c'(\theta)$	$B_c'(-\theta)$
.01	.00016396	3049.6531	.00016313	−.00016584
.02	.00065824	759.7244	.00064789	−.00066740
.03	.00147872	337.8503	.00144733	−.00151013
.04	.00262640	190.0859	.00254990	−.00270293
.05	.00409865	121.6865	.00395448	−.00425326
.06	.00589397	84.5335	.00564338	−.00616219
.07	.00800834	62.1331	.00761140	−.00843337
.08	.01043897	47.5935	.00984880	−.01106986
.09	.01318222	37.6255	.01234537	−.01409215
.10	.01623377	30.4951	.01509045	−.01747868
.11	.01958816	25.2195	.01808371	−.02124986
.12	.02324054	21.2069	.02129302	−.02540972
.13	.02718508	18.0839	.02472897	−.02994920
.14	.03141512	15.6059	.02836850	−.03486843
.15	.03592419	13.6067	.03221347	−.04018163
.16	.04070486	11.9704	.03622296	−.04587536
.17	.04574965	10.6141	.04042975	−.05196453
.18	.05105015	9.4775	.04477440	−.05844997
.19	.05659785	8.5155	.04927646	−.06531394
.20	.06238383	7.6940	.05392453	−.07255361
.21	.06839860	6.9870	.05868744	−.08018519
.22	.07463217	6.3740	.06355095	−.08820714
.23	.08107431	5.8392	.06852173	−.09650639
24	.08771443	5.3697	.07358761	−.10534803
.25	.09454171	4.9552	.07871368	−.11447916
.26	.10154433	4.5876	.08393175	−.12398616
.27	.10871084	4.2599	.08915963	−.13384062
.28	.11602911	3.9666	.09445423	−.14406030
.29	.12348653	3.7030	.09975445	−.15461454
.30	.13107048	3.4651	.10507142	−.16554699
.31	.13876802	3.2498	.11039236	−.17677381
.32	.14656568	3.0542	.11570450	−.18833816
.33	.15444990	2.8760	.12096765	−.20023248
.34	.16240676	2.7131	.12619550	−.21244845
.35	.17042214	2.5639	.13140382	−.22494899
.36	.17848181	2.4267	.13652381	−.23775218
.37	.18657103	2.3004	.14157095	−.25081902
.38	.19467518	2.1838	.14653297	−.26416757
.39	.20277919	2.0758	.15139772	−.27778706
.40	.21086781	1.9757	.15615323	−.29166617
.41	.21892595	1.8827	.16078772	−.30576255
.42	.22693804	1.7960	.16528960	−.32009385
.43	.23488851	1.7152	.16964753	−.33461420
.44	.24276176	1.6396	.17388165	−.34937896
.45	.25054171	1.5687	.17791877	−.36430560
.46	.25821271	1.5023	.18177938	−.37941344
.47	.26575877	1.4399	.18548491	−.39465644
.48	.27316376	1.3811	.18896210	−.41008308
.49	.28041166	1.3256	.19226473	−.42561485

If an arbitrary admittance $Y_L = A_L + jB_L$ is used to terminate the circuit at reference plane (1d) of Fig. 1, then the input admittance at reference surface (1c) normalized to the radial line characteristic admittance at r_2, defined by (5),

$$\frac{Y_{\text{radial}}}{Y_{\text{uniform}}} = \frac{\sin\theta}{\theta}, \tag{5}$$

is given by the expressions [3]

$$Y_{1c} = A_{1c} + jB_{1c} \tag{6a}$$

$$A_{1c} = \frac{\theta}{\sin\theta}\,\frac{A_L(B_b')^2}{x^2A_L^2 + (B_b' - x^2B_a' - xB_L)^2} \tag{6b}$$

$$B_{1c} = \frac{\theta}{\sin\theta}\left[xB_c' + \frac{B_b'(B_a' + xB_L)(B_b' - xB_L - x^2B_a') - A_L^2xB_b'}{x^2A_L^2 + (B_b' - x^2B_a' - xB_L)^2}\right] \tag{6c}$$

where B_a', B_b' and B_c' are obtained as follows by substituting in (1), (2), and (3):

$$b = x\frac{\lambda_g\sin\theta}{2\pi}. \tag{7}$$

We obtain

$$B_a = x\frac{\sin\theta}{\theta}\ln\frac{\theta}{\sin\theta} = xB_a'(\theta) \tag{8a}$$

$$B_b = \frac{1}{x}\,\frac{2}{\theta}\,\frac{\sin\theta}{1-(\sin 2\theta)/2\theta} = \frac{1}{x}B_b'(\theta) \tag{8b}$$

$$B_c = x\frac{\sin\theta}{\pi}\left[0.577 + \psi\left(\frac{\theta}{\pi}\right)\right] = xB_c'(\theta). \tag{8c}$$

From

$$b_2 = y\frac{\lambda_g\sin\theta}{2\pi} \tag{9a}$$

$$\theta_2 = -\theta \tag{9b}$$

$$\psi\left(\frac{\theta_2}{\pi}\right) = \psi\left(\frac{-\theta}{\pi}\right) = \psi\left(1-\frac{\theta}{\pi}\right) - \frac{1}{1-(\theta/\pi)}. \tag{10}$$

Substituting (9a), (9b), and (10) in (7), (8a), (8b), and (8c), we obtained the following relationships used in the computations (normalized to rectangular waveguide of height b_2):

$$B_{a_2} = -y\frac{\sin\theta}{\theta}\ln\frac{\theta}{\sin\theta} = -yB_a'(\theta) \tag{11a}$$

$$B_{b_2} = -\frac{1}{y}\,\frac{2}{\theta}\,\frac{\sin\theta}{1-(\sin 2\theta)/2\theta} = -\frac{1}{y}B_b'(\theta) \tag{11b}$$

$$B_{c_2} = y\frac{\sin\theta}{\pi}\left[0.577 + \psi\left(1-\frac{\theta}{\pi}\right) - \frac{1}{1-\theta/\pi}\right] = yB_c'(-\theta) \tag{11c}$$

where $B_a'(\theta)$, $B_b'(\theta)$, $B_c'(\theta)$, and $B_c'(-\theta)$ are tabulated in Table I.

In the case of a single filter section terminated in a matched waveguide (*i.e.*, a normalized real terminating admittance of unity value) the above equations reduce to

$$Y_{1c} = A_{1c} + jB_{1c} \tag{12a}$$

$$A_{1c} = \frac{\theta}{\sin\theta}\,\frac{(B_b)^2}{x^2 + (B_b' - x^2B_a')^2} \tag{12b}$$

$$B_{1c} = \frac{\theta}{\sin\theta}x\left[B_c' + \frac{B_a'B_b'(B_b' - x^2B_a') - B_b'}{x^2 + (B_b' - x^2B_a')^2}\right]. \tag{12c}$$

At reference surface (2d), the input admittance normalized to the radial line characteristic admittance at r_2 is

$$Y_{2d} = A_{2d} + jB_{2d} \tag{13a}$$

$$A_{2d} = \frac{A_{1c}\zeta(x, y)[1 + \text{ct}\,(x, y)\ \text{Ct}\,(x, y)]}{A_{1c}^2 + [\text{Ct}\,(x, y) - B_{1c}]^2} \tag{13b}$$

$$B_{2d} = \zeta(x_1 y)\ \frac{[\text{Ct}\,(x, y) - B_{1c}][B_{1c}\,\text{ct}\,(x, y) + 1] - A_{1c}^2\,\text{ct}\,(xy)}{A_{1c}^2 + [\text{Ct}(x, y) - B_{1c}]^2}\,. \tag{13c}$$

The radial functions are defined

$$\text{ct}(x, y) = \frac{J_1(x)N_0(y) - N_1(x)J_0(y)}{J_0(x)N_0(y) - N_0(x)J_0(y)} \tag{14a}$$

$$\text{Ct}(x, y) = \frac{J_1(y)N_0(x) - N_1(y)J_0(x)}{J_1(x)N_1(y) - N_1(x)J_1(y)} \tag{14b}$$

$$\zeta(x, y) = \frac{J_0(x)\text{N}_0(y) - N_0(x)J_0(y)}{J_1(x)N_1(y) - N_1(x)J_1(y)}\,. \tag{14c}$$

The admittance at reference plane (2c), normalized to the enlarged waveguide, is given by

$$Y_{2c} = A_{2c} + jB_{2c} \tag{15a}$$

$$A_{2c} = \frac{(\sin\theta/\theta)A_{2d}(B_b')^2}{y^2((\sin\theta/\theta)A_{2d})^2 + [B_b' + y^2B_c'(-\theta) + y(\sin\theta/\theta)B_{2d}]^2} \tag{15b}$$

$$B_{2c} = -yB_a' + \frac{B_b'[yB_c'(-\theta) + (\sin\theta/\theta)B_{2d}][B_b' + y^2B_c'(-\theta) + y(\sin\theta/\theta)B_{2d}] - yB_b'((\sin\theta/\theta)A_{2d})^2}{y^2((\sin\theta/\theta)A_{2d})^2 + [B_b' + y^2B_c'(-\theta) + y(\sin\theta/\theta)B_{2d}]^2}\,. \tag{15c}$$

Y_{2c} is computed and tabulated in Table II for $\theta = 45°$. At reference plane (2b), the input admittance normalized to the enlarged uniform waveguide is given by

$$Y_{2b} = A_{2b} + jB_{2b} \tag{16a}$$

$$A_{2b} = \frac{A_{2c}(1+\tan^2\phi)}{(A_{2c}^2+B_{2c}^2)\tan^2\phi - 2B_{2c}\tan\phi + 1} \tag{16b}$$

$$B_{2b} = \frac{(A_{2c}^2+B_{2c}^2-1)(-\tan\phi) + B_{2c}(1-\tan^2\phi)}{(A_{2c}^2+B_{2c}^2)\tan^2\phi - 2B_{2c}\tan\phi + 1} \tag{16c}$$

$$\phi = 2\pi l_1/\lambda_g \tag{16d}$$

where l_1 is shown on Fig. 3.

The input admittance at reference plane (2a), normalized to the enlarged uniform waveguide, is

$$Y_{2a} = A_{2a} + jB_{2a} \tag{17a}$$

$$A_{2a} = \frac{A_{2b}(B_b')^2}{y^2A_{2b}^2 + (B_b' - y^2B_a' + yB_{2b})^2} \tag{17b}$$

$$B_{2a} = yB_c'(-\theta) + \frac{yA_{2b}^2B_b' - B_b'(yB_a' - B_{2b})(B_b' - y^2B_a' + yB_{2b})}{y^2A_{2b}^2 + (B_b' - y^2B_a' + yB_{2b})^2}\,. \tag{17c}$$

Using the normalizing relationship equation (5), the input admittance normalized to the radial line at reference plane (1b) is

$$Y_{1b} = A_{1b} + jB_{1b} \tag{18a}$$

$$A_{1b} = \frac{(\theta/\sin\theta)A_{2a}\zeta(x, y)[1 + \text{Ct}\,(x, y)\ \text{ct}\,(x, y)]}{((\theta/\sin\theta)A_{2a})^2 + [\zeta(x, y)\ \text{ct}\,(x, y) - (\theta\sin\theta)B_{2a}]^2} \tag{18b}$$

$$B_{1b} = \frac{[\zeta(x, y) + (\theta/\sin\theta)B_{2a}\ \text{Ct}\,(x, y)]\ [\zeta(x, y)\text{ct}\,(x, y) - (\theta/\sin\theta)B_{2a}) - ((\theta\sin\theta)A_{2a})^2\ \text{Ct}\,(x, y)]}{((\theta/\sin\theta)A_{2a})^2 + [\zeta(x, y)\ \text{ct}\,(x, y) - (\theta/\sin\theta)B_{2a}]^2}\,. \tag{18c}$$

It is now possible to obtain the input admittance in the normal waveguide of the over-all filter using the normalizing relationship equation (5) at reference plane (1a).

$$Y_{1a} = A_{1a} + jB_{1a} \tag{19a}$$

$$A_{1a} = \frac{(\sin\theta/\theta)A_{1b}(B_b')^2}{x^2((\sin\theta/\theta)A_{1b})^2 + (B_b' - x^2B_c' - x(\sin\theta/\theta)B_{1b})^2} \tag{19b}$$

$$B_{1a} = xB_a' + \frac{B_b'(B_c' + (\sin\theta/\theta)B_{1b})(B_b' - x^2B_c' - x(\sin\theta/\theta)B_{1b}) - xB_b'((\sin\theta/\theta)A_{1b})^2}{x^2((\sin\theta/\theta)A_{1b})^2 + (B_b' - x^2B_c' - x(\sin\theta/\theta)B_{1b})^2}\,. \tag{19c}$$

From the input admittance we obtain over-all insertion loss of the filter section:

$$\frac{P_{\text{out}}}{P_{\text{in}}} = a = \frac{4A_{1a}}{(1 + A_{1a})^2 + B_{1a}^2}\,. \tag{20}$$

Design Procedure

The procedure and examples to be indicated here will assume tapers of 45° (between wall of radial line and center line), since this is considered the most useful compromise between power handling capacity and

TABLE II

INPUT ADMITTANCE OF 45° STEP-DOWN TAPER WITH MATCHED OUTPUT

y \ x	0.5	0.6	0.7	0.8	0.9	1.0	1.1
→ 0.6	1.203338						
0.7	1.400145	1.171531					
0.8	1.584169	1.336229	1.149481				
0.9				1.133411			
1.0				1.257456	1.122035		
1.1				1.376837	1.232227	1.113286	
1.2	1.892920	1.797739	1.646330	1.485810	1.339045	1.212427	1.106944
1.3							
1.4							
A_{2c} 1.5							
1.6	1.436203	1.601366	1.680624	1.681639	1.627135	1.540339	1.440697
1.7							
1.8							
2.0	.956902	1.139597	1.303417	1.434964	1.524405	1.567949	1.568651
2.4	.686599	.818574	.952227	1.083890	1.207538	1.316435	1.402999
2.8	.555438	.647212	.741529	.839086	.938822	1.039214	1.136668
3.2	.505724	.570511	.635659	.703110	.773405	.847202	.923858
3.6	.514265	.557999	.600448	.644019	.689656	.738529	.790976
4.0	.582900	.603380	.622911	.643958	.667319	.693994	.724410
4.4	.738647	.720488	.707358	.700096	.698189	.701612	.710193
→ 4.8	1.047913	.947917	.875883	.823862	.786338	.760096	.743106
→ 0.6	−.0155465						
0.7	−.0483493	−.0160211					
0.8	−.123856	−.0382917	−.0170323				
0.9				−.0191752			
1.0				−.0300653	−.0210976		
1.1				−.0632006	−.0280343	−.0229026	
B_x 1.2	−.778274	−.459627	−.247148	−.120734	−.0541517	−.0269147	.0249325
1.3							
1.4							
1.5							
1.6	−1.202105	−.984238	−.748404	−.528785	−.347814	−.212308	−.120243
1.7							
1.8							
2.0	−1.098445	−1.053025	−.967434	−.846537	−.703159	−.552165	−.409345
2.4	−.816035	−.845162	−.853190	−.836469	−.794072	−.726502	−.638047
2.8	−.505030	−.562132	−.608420	−.641609	−.659958	−.661280	−.643980
3.2	−.193129	−.265097	−.329102	−.384583	−.431033	−.467416	−.492219
3.6	+.118990	+.0328891	−.0439492	−.112515	−.173470	−.227077	−.272838
4.0	+.432248	+.327315	+.236413	+.156395	+.0852311	+.0214090	−.0355494
4.4	+.737174	+.606920	+.499452	+.407806	+.327947	+.256887	+.193178
→ 4.8	+.980700	+.831424	+.713496	+.615469	+.531509	+.457437	+.391136

y \ x	1.2	1.3	1.4	1.5	1.6	1.7	1.8
→ 1.3	1.102315						
1.4	1.184604	1.099170					
1.5	1.264938	1.174456	1.096732				
1.6	1.341129	1.248624	1.166336	1.095743			
A_{2c} 1.7					1.095495		
1.8					1.155230	1.095610	
2.0	1.535852	1.480423	1.412644	1.341301	1.271392	1.206468	1.148527
2.4	1.462342	1.492353	1.494659	1.474178	1.436856	1.389098	1.336240
2.8	1.227035	1.305527	1.367826	1.410693	1.433332	1.436809	1.423382
3.2	1.002140	1.080043	1.154927	1.223157	1.281993	1.328638	1.360688
3.6	.846932	.906034	.967494	1.029482	1.090638	1.148711	1.200977
4.0	.758646	.796790	.838723	.883641	.931199	.980305	1.029519
4.4	.723529	.741489	.763899	.790229	.820372	.853773	.889868
→ 4.8	.733640	.730716	.733574	.741467	.754008	.770671	.791189
→ 1.3	−.0267145						
1.4	−.0260050	−.0283318					
1.5	−.0381399	−.0260197	−.0300578				
1.6	−.0638222	−.0348989	−.0261142	−.0314047			
1.7					−.0326896		
B_{2c} 1.8					−.0260868	−.0334130	
2.0	−.285833	−.187433	−.115042	−.0666671	−.0382406	−.0256887	−.0257226
2.4	−.536137	−.429640	−.327248	−.236580	−.161207	−.102821	−.0615519
2.8	−.608091	−.554937	−.487734	−.412044	−.333050	−.256506	−.187408
3.2	−.504372	−.502659	−.486625	−.456893	−.414759	−.362990	−.305088
3.6	−.310386	−.338874	−.357444	−.365389	−.362252	−.348144	−.323434
4.0	−.0860780	−.130078	−.167284	−.197094	−.219146	−.232962	−.237769
4.4	+.135687	+.0838508	+.0373597	−.00355278	−.0389994	−.0686821	−.0918718
→ 4.8	+.331088	+.276328	+.226202	+.180699	+.139349	+.102214	+.0697134

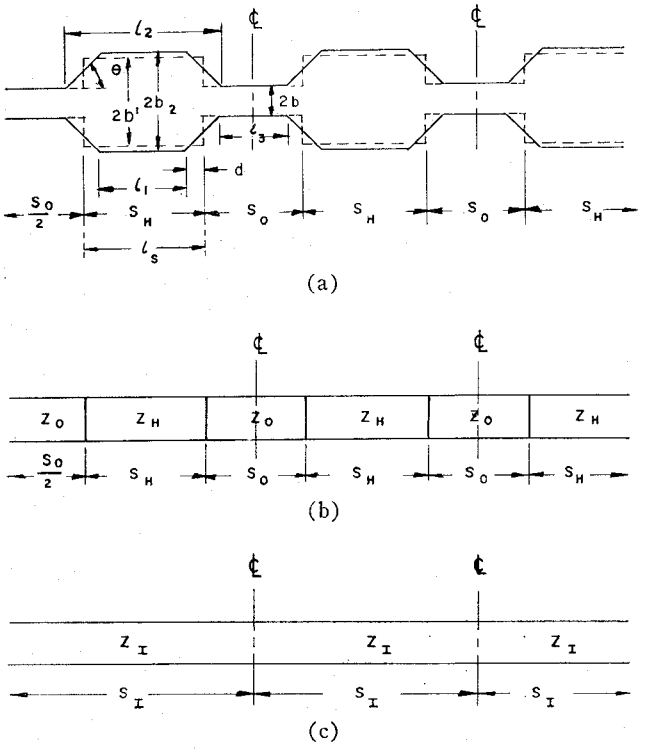

Fig. 3—Physical dimension. (a) Equivalent circuit. (b) Equivalent iterative cell. (c) Multiple section filter.

maximum effective discontinuities. Since (r_2-r_1) and l_1 are independent variables, the frequencies of minimum and maximum insertion loss can be specified to obtain two sets of simultaneous equations (5) to (20) which can be solved to give the required length and height. While the preceding statement is true in principle, the actual reduction to practice is not practical without a high-speed computer since the equations are complex combinations of Bessel and transcendental functions. The problem can be solved without a computer, however, by the use of equivalent steps which will considerably simplify the design procedure and calculations, and produce fairly accurate results.

It can be shown that for every radial line section terminated at each end in a uniform waveguide, there exists an equivalent step which is a function of frequency [3]. The design procedure can then be carried out using uniform waveguide of enlarged E-plane dimensions (guide height) connected by steps, and the equivalent taper section can be determined to complete the design.

A plot of the input admittance of a step-down taper terminated in a match obtained from Table II will show that the VSWR in general varies inversely with the frequency. "Step-down" denotes the case where the wave propagates from a larger to smaller guide. As y is made larger, the VSWR gets smaller (Fig. 4), and only at one point on each curve (one frequency), can the magnitude of the admittance be approximated by the ratio of the heights. This characteristic introduces another computational problem when iterative sections

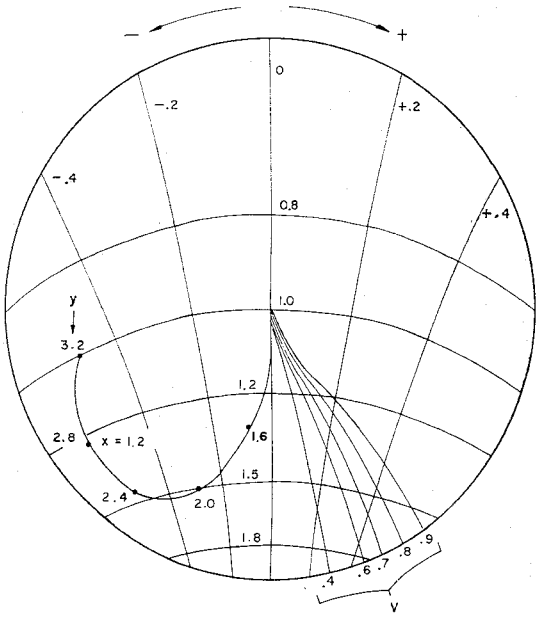

Fig. 4—Plot of input admittance for taper terminated in match ($x=1.2$) as a function of y.

are used to design a filter. While the frequency response of a single section can be computed directly from the radial line equation, the computation of an iterative structure of a number of sections is virtually impossible without the use of a high-speed, large capacity digital computer. To overcome the need for a large computer, the concept of the equivalent step is introduced to permit the use of the simplified equivalent circuit and equivalent iterative cell of Fig. 3. By means of the equivalent step, a design procedure for an iterative filter becomes possible.

The Equivalent Step

Since we have normalized the radial line relationships in terms of x and y as previously defined by (4a) and (4b), we will similarly normalize the step characteristics to U and V.

$$U = b'/b \tag{21}$$

where $2b'$ is the height of the enlarged equivalent waveguide (Fig. 3) and $2b$ is the height of the standard waveguide.

$$V = b'/\lambda_g = Ub/\lambda_g \tag{22}$$

Since the standard size guide is the same for both the input to the taper section and the equivalent step section, the ratio of V to U can be expressed in terms of x:

$$\frac{V}{U} = x\,\frac{\sin\theta}{\pi}\,. \tag{23}$$

For 45° tapers, we get

$$\frac{V}{U} = 0.22508x. \tag{24}$$

The output radial line section, the equivalent step, and their equivalent circuits are shown in Fig. 2.

The normalized input admittance in the large guide at the step of a step down terminated in a load Y_L, normalized to the output guide, is given by the expression

$$Y = (b'/b)Y_L + jB/Y_{01} \tag{25}$$

where B/Y_{01} is the discontinuity susceptance due to the step normalized to the output guide [10].[1] If a matched output load is considered, then (25) reduces to

$$Y = b'/b + jB/Y_{01} = U + jB/Y_{01}. \tag{26}$$

Thus, if we plot on a Smith Chart the input admittance for the step down with matched output, the value of U can be determined directly since it is identical with the conductance (real part) of the admittance.

One can always select a step designed by U and V with an insertion VSWR equal to that of a specific taper. The input admittance plotted on a Smith Chart for either the taper or step will move around the constant VSWR circle in the same manner when the input reference planes are moved identical electrical distances. The input admittance for the step is specified in the plane of the step. The input admittance for the taper is specified at the junction of the enlarged waveguide and the radial line. The angular displacement on the constant VSWR circle between the two input admittances corresponds to the distance in fractions of a waveguide wavelength between the taper and the equivalent step.

In order to permit graphical computation of a filter, the input admittances for a family of selected step down tapers have been computed on a digital computer from (5) to (15), and are tabulated in Table II. The input admittances for the step (step down) have been plotted on Fig. 4 for selected values of V with U as the continuous variable. These are the curves to the right of the real axis on the Smith Charts. The input admittance of a step of height ratio U can be found where the conductance curve, equal in magnitude to U, intersects the curve for the appropriate V. The plotted curves correspond to $V=0.4$, 0.6, 0.7, 0.8, and 0.9 going from the real axis to the right. For selected values of y/x the input admittance can be plotted with x as the continuous variable. The insertion VSWR curve which intersects with the input admittance curve of a fixed step down increases as the frequency increases (x grows larger). The taper, however, shows a generally decreasing VSWR as x and y increase. The insertion VSWR must be the same for the taper and its equivalent step, and this equivalent step will be a valid approximation only over a narrow frequency band. However, for very small steps and corresponding tapers, the bandwidth, over which the step is a valid approximation, will be larger as the step gets smaller. For a given step the susceptance increases if the wavelength is made shorter. The taper, however, acts like an impedance matching structure between the larger and smaller height waveguides, and the match gets progressively better for shorter wavelengths.

[1] See Marcuvitz [1], pp. 307–309.

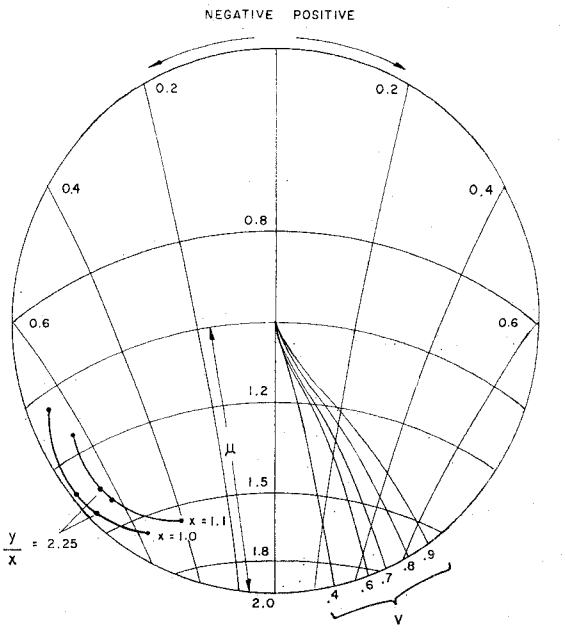

Fig. 5—Plot of input admittance for taper terminated in match ($x=1.1$, $x=1.0$) as a function of y.

Procedure for Determining Equivalent Step

The procedure for determining equivalent steps can best be described by an illustrative example. This approach is not necessary for a single section, but will be used later in the design of an iterative filter.

A requirement is given for a section of a filter that has a maximum insertion loss at 10,320 mc and a zero insertion loss at 9500 mc. The pass band is to be essentially symmetrical. From the frequencies we readily compute the waveguide wavelengths in the standard 1 inch$\times\frac{1}{2}$ inch rectangular waveguide (0.900$\times$0.400 inches ID). A frequency of 9500 mc corresponds to a waveguide wavelength of 4.451 cm and 10,320 mc to a waveguide wavelength of 3.762 cm. From the waveguide wavelengths and the height of the standard waveguide (1.016 cm), the values of x are obtained from (4b). For 9500 mc, $x=1.014$; and for 10,320 mc, $x=1.2$. The values of input admittance from Table II have been plotted on a Smith Chart (Fig. 4). From this curve and Table II the desired value of y/x can be determined. A value of $y=2.70$ is selected which will give the maximum discontinuity at $x=1.2$. This gives a value of y/x of 2.25. The next step in the procedure is to obtain the equivalent step from the value of the discontinuity, Y_{2e}, resulting from a matched output step-down taper of y/x of 2.25 at $x=1.014$. This may be calculated by means of (5), (11), (13), and (15) or graphically by plotting from Table II the values for $x=1$ and $x=1.1$ as y varies from 2 to 2.8. This is shown on Fig. 5. From the plotted value of Y_{2e}, a constant VSWR circle is drawn so as to intersect the input admittance curves of the equivalent output matched step.

The values on the constant VSWR circle are:

$$V = 0 \qquad U = 1.94$$
$$V = 0.4 \qquad U = 1.875$$
$$V = 0.6 \qquad U = 1.78.$$

From (24), we find that the relationship between U and V for $x=1.014$ should be $V/U=0.22823$ for identical output waveguides for both step and taper. From the values of V and U, we find respectively the ratios V/U of 0, 0.21333, and 0.33708. Since U, V and V/U are monotonic and continuous over the region of interest, the desired value U and V along the constant VSWR circle can be found to give the required ratio of V/U. $V/U=0.22823$ lies between that corresponding to $V=0.4$, $U=1.875$ and $V=0.6$, $U=1.78$. Linear interpolation gives a value of $U=1.86$ and a corresponding $V=0.425$ which prove to be the desired values corresponding to $V/U=0.22823$. If the first linear interpolation had resulted in a value of V/U different from that required, interpolation could have been repeated between the two new values of V/U on either side of the desired value. From the values of U and V, we find from the Smith Chart the input admittance of the output matched step to be $1.86+j.32$. The phase angle traversed in going from the input admittance of the taper $A_{2c}+jB_{2c}$ to the input admittance of the equivalent step $A_{2b}+jB_{2b}$ is the distance (d) toward the generator from reference plane (2c) of the taper to the plane of the equivalent step discontinuity. The equivalent step may now be used to obtain the line length (l_1) required to give a match at $\lambda_g=4.451$. From the Smith Chart, this is found to be $\lambda_g/2$ plus $0.038\lambda_g$, *i.e.*, $0.538\lambda_g$ for the equivalent step. To obtain the spacing required for the taper section, the distance (d) traversed along the constant VSWR circle is found to be $0.0805\lambda_g$. Since the equivalent step and the taper are symmetrical about the same center line the length of the enlarged uniform waveguide is obtained from the following relationship (Fig. 3):

$$l_1 = l_s - 2d. \tag{27}$$

In this example l_1 is found to be $0.377\lambda_g=1.500$ cm. All the necessary dimensions have now been obtained, *i.e.*, $b_2=2.286$ cm, $l_1=1.500$ cm and $\theta=45°$.

The insertion loss may now be calculated at any frequency by finding λ_g and x in turn, and obtaining graphically the equivalent step and the distance, d (traversed in going from the taper input admittance to the equivalent step input admittance). Using (27) where l_1 is the physical length of the enlarged waveguide between tapers, l_s can be obtained. The Smith Chart can be used to obtain the input admittance $A_{2a}+jB_{2a}$, due to the equivalent step at a distance l_s toward the generator from the plane of the step. The input admittance Y_s in the standard guide of the matched output filter section can be obtained from the relationship

$$Y_s = \frac{1}{U}\left[A_{2a} + j(B_{2a} + B_{2b})\right] \tag{28}$$

$$Y_s = A_s + jB_s. \tag{29}$$

The insertion loss α_s can be obtained from

$$a_s = \frac{4A_s}{(1 + A_s)^2 + B_s^2}. \tag{30}$$

The values of insertion loss obtained by the equivalent step method for the single section previously considered are plotted on Fig. 6 together with the curve obtained from plotting the insertion loss using (5) through (20). The measured insertion loss is also plotted on the same curve. This shows that the equivalent step is a fairly good approximation.

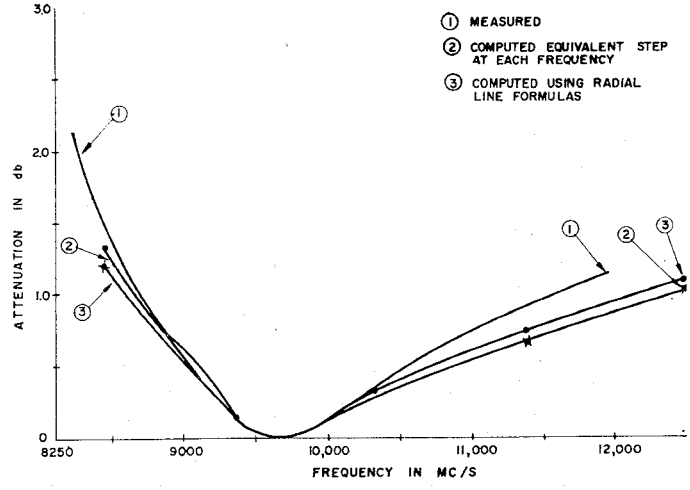

Fig. 6—Comparison of computed and measured insertion loss for single filter section.

The Multiple Section Filter

To obtain high-power microwave filter structures to meet specific requirements, a number of sections are required. The multiple section procedure follows from the procedure for a single section. Using Fig. 3(a), the multiple section filter can be described in terms of the taper angle θ and the lengths l_1, l_2, and l_3. From the single taper section, using the procedure previously described, the equivalent step parameters U, V, and d may be found for each frequency. From these the values Z_H, S_H, and S_O are determined by the relationships

$$S_H = l_1 + 2d \tag{31}$$

$$S_O = l_3 + 2(b_2 - b)\cot\theta - 2d \tag{32}$$

$$Z_H/Z_O = U = b'/b \tag{33}$$

where Z_H and Z_O are the characteristic impedances shown in Fig. 3.

The following relationships developed by J. W. E. Griemsmann will give the equivalent iterative cell, corresponding to the equivalent step structure [Fig. 3(b) and 3(c)]. The normalized equivalent impedance is

$$\left(\frac{Z_I}{Z_O}\right)^2=\frac{\tan\left[\beta(S_O/2)+\tan^{-1}\left((Z_H/Z_O)\tan\beta(S_H/2)\right)\right]}{\tan\left[\beta(S_O/2)+\tan^{-1}\left((Z_O/Z_H)\tan\beta(S_H/2)\right)\right]} \quad (34)$$

and the phase change per section βS_I is then

$$\cos\beta S_I = \cos\beta S_H\cos\beta S_O - \tfrac{1}{2}\left((Z_H/Z_O)+(Z_O/Z_H)\right)\sin\beta S_H\sin\beta S_O \quad (35a)$$

$$\beta = 2\pi/\lambda_g. \quad (35b)$$

Using the results of (34) and (35) the reciprocal of the insertion loss can be obtained for n sections at the specified frequency (or waveguide wavelength) by [4]

$$\frac{1}{a_n}=\frac{P_{\text{in}}}{P_{\text{out}}}=1+\frac{1}{4}\left(Z_I-\frac{1}{Z_I}\right)^2\sin^2 n\beta S_I. \quad (36)$$

Since taper sections cannot be approximated directly by change in impedance alone, the above procedure for finding the equivalent iterative cell requires the determination of the equivalent step sections at each frequency.

Design Procedure and General Considerations

A band-pass band-elimination filter suitable for this type of high-power structure is specified in terms of the lower cutoff frequency, the upper cutoff frequency, the width of the attenuation band at the high-frequency end, and the steepness of the rise of insertion loss just beyond the cutoff frequencies of the filter.

The cutoff wavelength of the standard uniform waveguide used in the structure determines in large measure the slope of the insertion loss at the lower end of the pass band. If the specified lower frequency cutoff is close to the guide cutoff, this characteristic can easily be used to achieve the required low-frequency slope. In general, spurious responses will exist in the filter structure due to the repetitive nature of the waveguide circuit elements. The locations of these spurious responses depend on the steepness of the rise of the insertion loss just beyond the cutoff frequency of the filter and on the electrical lengths of the various circuit elements used in the filter. Since the pass band may repeat at half the waveguide wavelength of the design pass band, it is necessary to use various devices to increase the width of the rejection band at the high end. One convenient method of eliminating spurious responses under such circumstances is to design a composite filter made up of several dissimilar filters so that the pass bands are the same but the frequency of infinite insertion are sufficiently different so that the spurious pass band of one filter coincides with the rejection band of another.

Illustrative Examples

The design procedure can be considered in terms of a specific filter. The problem is to design a 1 inch $\times\frac{1}{2}$ inch waveguide filter with a pass band from 8200 to 10,100 mc, with an insertion loss of greater than 25 db below 8100 mc and also between 10,200 and 10,850 mc. This specification is in keeping with the expectation of a spurious pass band at half the design waveguide wavelength, so only one filter need be designed. If a broader rejection band had been specified, additional dissimilar filters would be needed. Converting the specifications to waveguide wavelength gives us the cutoff wavelengths of 6.088 and 3.902 cm, respectively, and the 25-db insertion loss waveguide wavelengths of 6.303, 3.837, and 3.468 cm, respectively.

From the above values, wavelengths of infinite insertion loss and the wavelengths of zero insertion loss must be selected. For the high-frequency rejection band a central wavelength should be selected, *i.e.*, 3.700 cm (10,400 mc). To obtain the desired low-frequency cutoff and slope of insertion loss, the frequency of zero insertion loss must be selected in combination with the height of the enlarged waveguide to give the desired symmetry. Since the filter to be designed has a very large pass band, it is necessary to use a taper section y/x ratio which shows a relatively slow variation of impedance with wavelength. Examination of Table II shows $y/x=2$ has a curve of the required type. It is now necessary to find x (4a) corresponding to the cutoff wavelengths and the infinite insertion wavelengths. The cutoff wavelengths give values of x of 0.741 and 1.157, respectively. The wavelength for infinite insertion loss gives a value of x of 1.220. A central value of $x=1.0$ ($\lambda_g=4.514$ cm) is selected as the wavelength of zero insertion loss. The 25-db points occur at values of x of 0.716 and 1.302, respectively.

For minimum insertion loss in the pass band (where the pass band is broad) using identical sections, each section is matched at the center frequency (zero insertion loss). Using the procedure outlined in the single-filter section, we find the equivalent step corresponding to $y/x=2$ and $x=1$. The resultant values are $U=1.82$, $V=0.4$, and $d=0.0381\lambda_g$. From the Smith Chart, the length l_s is found to be $\lambda_g/2$ plus $0.039\lambda_g$, *i.e.*, $l_s=0.539\lambda_g$ $=2.433$ cm. Eq. (27) is used to obtain the value of the length of the enlarged waveguide l_1. This value is found to be 1.761 cm. The next step in the procedure is the determination of the distance between the sections [l_3 of Fig. 3(a)] to give the desired rejection band. For the upper rejection band the 25 db insertion loss wavelengths are 3.837 cm ($x=1.176$) and 3.468 cm ($x=1.302$), respectively. Select a second cutoff at 3.30 cm. The procedure is to find the value of S_O from (34), which will make $(Z_I/Z_O)^2$ infinite at the first cutoff wavelength of 3.902 cm and zero at 3.30 cm, corresponding to the limits of the attenuation band of the filter. To do this, it is necessary to find the equivalent step using the procedure given before corresponding to $x=1.157$ and 1.368, respectively, and determining U, V, and d for each. Using (31), S_H is obtained for each value of x. The following equations can now be used to obtain the value of S_O for the lower and upper frequencies ($x=1.157$ and $x=1.368$), respectively:

$$\beta \frac{S_O}{2} = -\tan^{-1}\left((Z_O/Z_H)\tan\beta(S_H/2)\right) + n\pi \quad (37)$$

$$\beta \frac{S_O}{2} = -\tan^{-1}\left((Z_H/Z_O)\tan\beta(S_H/2)\right) + n\pi \quad (38)$$

where Z_H/Z_O is defined by (33). The results of (37) and (38) when inserted in (32) should give approximately the same value of l_3. If this is not the case, the original choices of y/x and of the zero insertion loss wavelength must be modified. For a fixed zero insertion loss wavelength, the larger y/x will result in greater rejection bandwidth, but the lower frequency cutoff will go to higher frequency. This can be compensated by lowering the frequency of zero insertion. S_O at the lower cutoff of $\lambda_g = 6.088$ should satisfy (30). In this case, the conditions of (37) and (38) are satisfied by $l_3 = 0.785$ cm for the cutoff wavelengths of 6.088, 3.902, and 3.300 cm.

The design is essentially complete. From y/x we determine $b_2 = 2.032$ cm. The values $l_1 = 1.761$ cm and $l_3 = 0.785$ cm have been determined and $\theta = 45°$ has been specified for maximum power. It now remains to determine the total number of sections to be used in the filter to achieve the desired steepness of the rise of the insertion loss. Fig. 7 shows the insertion loss characteristics of 6, 15 and 21-section filters designed and built as outlined above. The 15-section unit almost meets the 25-db steepness requirement, and the 21-section unit has a steeper slope than specified. The cutoff frequencies occur as computed but the insertion loss in the pass band shows several peaks which do not agree. These may be due to machining tolerances or misalignments. When the rejection band is not too broad, an approximation which has been found empirically to be of relatively good accuracy is to select S_O which satisfies the following relationship at the infinite insertion loss wavelength:

$$S_O = \tfrac{1}{3}\lambda_{g\infty}. \quad (39)$$

The insertion loss of a multiple section filter in the pass band can be calculated from (31) through (36) using the equivalent step determined at each frequency by the method outlined in the single-filter section.

Summary of Procedure

The following steps are required to design a high-power filter with a specified pass band and rejection band.

1) Determine cutoff wavelengths for lower and upper ends of pass band and for upper end of rejection band.
2) Determine x as defined by (4b) for each cutoff wavelength.
3) Select value of y/x having desired type of frequency response.
4) Select wavelength of zero insertion loss to give symmetrical filter.

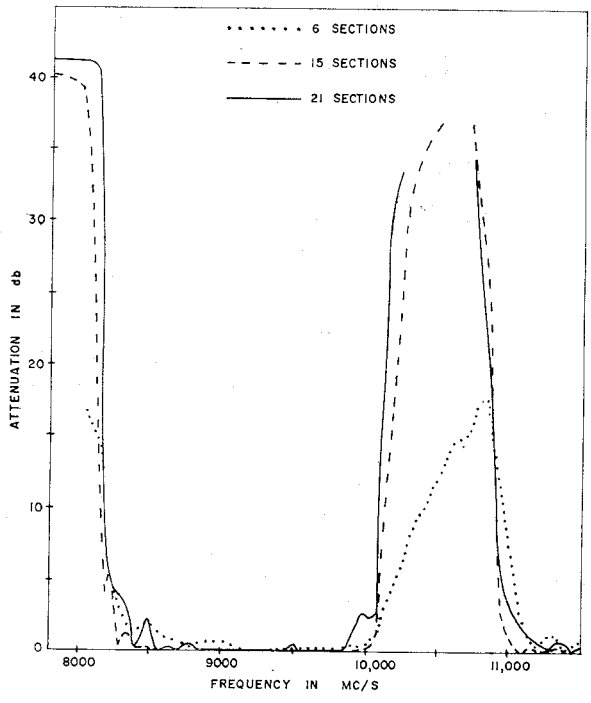

Fig. 7—Insertion loss of 6, 15, and 21-section filters.

5) Determine equivalent steps corresponding to taper of height y/x for zero insertion wavelength.
6) Find S_H length of step section which gives match at the wavelength of zero insertion loss.
7) Using (31) find l_1.
8) For the cutoff wavelengths on either side of the rejection band, find the equivalent steps corresponding to each, and calculate S_H from (31).
9) For the longer cutoff wavelength compute S_O from (37) and for the shorter cutoff wavelength from (38).
10) In each case, compute l_3 from (32).
11) If l_3 is not approximately equal in the two cases, choose a new value of y/x and repeat process.
12) Find equivalent step for the cutoff wavelength at the lower end of pass band and check that computed S_O satisfies (38). If it does not, the wavelength of zero insertion loss should be modified accordingly.
13) Compute b_2 from y/x and b_1, *i.e.*, $y/x = b_2/b_1$.
14) Select number of sections in accordance with the required steepness of rise of insertion loss.

Power Handling Capability

The power handling capacity of a waveguide structure is an inverse function of the maximum electric field gradient in the structure. To compare the power handling capacities of waveguide structures of equal width in the TE_{10} mode, it is necessary to examine the relative gradients in the structures. Using the method of curvilinear squares, the gradients have been obtained for the static equivalent of a radial line mated at both ends to uniform lines, and a step between uniform lines of dif-

ferent heights. The relative gradients have been determined by comparison at the 0.05 potential points relative to the smaller uniform line.

The results indicate a ratio of 3.0/1.8 for the gradient of the step compared to the 45° taper section. This analysis predicts a substantially larger power handling capacity for filters made up of taper sections. A series of measurements were made on single step and single taper sections of equal height with spacings between discontinuities to produce a low VSWR to obtain a comparison of power handling capacity. The measurements were made at 9450 mc using a magnetron of in excess of 700 kw of peak power in 1 inch by $\frac{1}{2}$ inch waveguide (normal average unpressurized breakdown power of 400 kw depending on humidity and ionization present). The power handling capacities of a 6-section and a 15-section radial line filter were also measured. The last filter section consisted of a step and a taper combined to give a relatively good VSWR at 9450 mc. Each filter was measured unpressurized, with 10 pounds per square inch pressure, and with 15 pounds pressure. The results were in keeping with the predictions from the comparison of the gradients in the two types of structures. The measured results follow in Table III.

TABLE III

Type of structure	Enlarged waveguide to std. waveguide ratio	Power when arcing started		
		No pressure	10 lbs. pressure	15 lbs. pressure
Single taper section	$b_2/b = 2.25$	340 kw	*700 kw	
Single step section	$b_2/b = 2.25$	40 kw	90 kw	140 kw
Six section taper filter	$b_2/b = 2.0$	140 kw	*700 kw	
Fifteen section taper filter	$b_2/b = 2.0$	250 kw	*700 kw	
Single section step and taper	$b_2/b = 3.5$	90 kw	90 kw	240 kw

No arcing occurred at maximum available power.

Discussion of Experimental Filters

The performance of the filter structure (Fig. 7) designed by using the preceding method, is very close to the expected performance. The 21-section filter was made in 2 parts, to fit the limits of the milling equipment available. One part consisted of 15 sections while the other consisted of 6 sections. An analytic computation of the 15-section filter, using the method outlined in the discussion of the multiple section filter, showed agreement within the actual machining tolerances except for the small insertion loss peaks from 8200 to 8500 mc. The measured insertion loss was within 0.1 db of the computed values in the pass band except at the low-frequency end. In the case of the 6-section filter there was a more marked disagreement between the measured insertion loss and the computed insertion loss below 9000 mc. This disagreement is also found when the 2 parts are put together to form the 21-element filter. Physical measurement of the individual sections of the 6-section filter was not possible without disassembly, but external measurement indicated a total length which was 0.010 inch beyond the tolerances shorter than specified. This would suggest that one or more of the individual sections differed considerably from the design dimensions. The structure would no longer be exactly iterative and the computed results would not be directly applicable. Both the high insertion loss section filter and the normal filter were subjected to 700 kw of peak power with 10 pounds pressurization without any sign of breakdown.

Bibliography

[1] N. Marcuvitz, "Waveguide Handbook," M.I.T. Rad. Lab. Ser., McGraw-Hill Book Co., Inc., New York, N. Y., vol. 10, pp. 322–323; 1951.
[2] E. Jahnke and F. Emde, "Tables of Functions," Dover Publications, New York, N. Y., 4th ed., p. 16; 1945.
[3] J. H. Vogelman, "High Power Filters," D.E.E. dissertation, Polytechnic Inst. Brooklyn, Brooklyn, N. Y.; 1957.
[4] G. L. Ragan, "Microwave Transmission Circuits," M.I.T. Rad. Lab. Ser., McGraw-Hill Book Co., Inc., New York, N. Y., vol. 9, pp. 643–715; 1948.
[5] Radio Res. Lab. Staff, "Very High Frequency Techniques," McGraw-Hill Book Co., Inc., New York, N. Y., vol. 2, pp. 674–678; 1947.
[6] S. Cohn, "Analysis of wide-band waveguide filter," Proc. IRE, vol. 37, pp. 651–656; June, 1949.
[7] S. Cohn, "Design relations for the wide-band waveguide filter," Proc. IRE, vol. 38, pp. 799–803; July, 1950.
[8] J. Greene, "Corrugated-waveguide band-pass filters," *Electronics*, vol. 24, pp. 117–119; July, 1951.
[9] E. N. Torgow, "Broadband waveguide filters," Polytechnic Inst. Brooklyn, Brooklyn, N. Y., Rep. R-447-55, PIB-377; October, 1955.
[10] C. G. Montgomery, R. W. Dicke, and E. M. Purcell, "Principles of Microwave Circuits," M.I.T. Rad. Lab. Ser., McGraw-Hill Book Co., Inc., New York, N. Y., vol. 8, pp. 187–188; 1948.